LANGMUIR

Article

pubs.acs.org/Langmuir

Discrimination of Proteins Using an Array of Surfactant-Stabilized Gold Nanoparticles

Jacob L. Rogowski,[†,‡] Mohit S. Verma,[†,‡] and Frank X. Gu*[,†,‡]

[†]Department of Chemical Engineering, University of Waterloo, 200 University Avenue West, Waterloo, Ontario N2L 3G1, Canada

[‡]Waterloo Institute for Nanotechnology, University of Waterloo, 200 University Avenue West, Waterloo, Ontario N2L 3G1, Canada

Supporting Information

ABSTRACT: Protein analysis is a fundamental aspect of biochemical research. Gold nanoparticles are an emerging platform for various biological applications given their high surface area, biocompatibility, and unique optical properties. The colorimetric properties of gold nanoparticles make them ideal for point-of-care diagnostics. Different aspects of gold nanoparticle−protein interactions have been investigated to predict the effect of protein adsorption on colloidal stability, but the role of surfactants is often overlooked, despite their potential to alter both protein and nanoparticle properties. Herein we present a method by which gold nanoparticles can be prepared in various surfactants and used for array-based quantification and identification of proteins. The exchange of surfactant not only changed the zeta potential of those gold nanoparticles but also drastically altered their aggregation response to five different proteins (bovine serum albumin, human serum albumin, immunoglobulin G, lysozyme, and hemoglobin) in a concentration-dependent manner. Finally, we demonstrate that varying surfactant concentration can be used to control assay sensitivity.

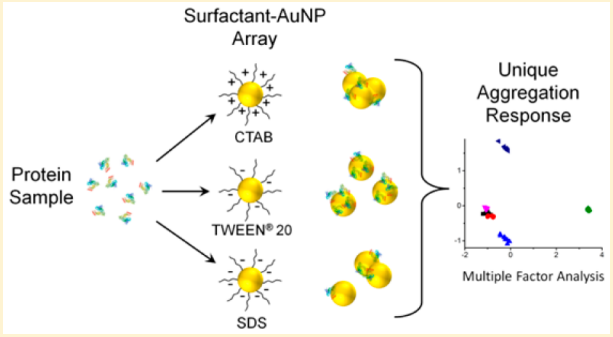

INTRODUCTION

Proteins play a vital role in countless biochemical and physiological processes. Variations in protein concentration or function can often be associated with ongoing biological process and overall health. Given their importance, the ability to detect and quantify proteins is a fundamental part of many bioanalytical and clinical investigations.[1−3] While several biochemical methods exist for protein quantification such as the Bradford, bicinchoninic acid (BCA), and Lowry assays, these colorimetric methods are not used for protein identification. The identification of proteins in solution is much more challenging than quantification. Gel-based assay such as polyacrylamide gel electrophoresis (PAGE) may provide an approximate size for a protein, but this alone cannot be used for conclusive identification because many polypeptides share similar molecular weights. Western blots and enzyme-linked immunosorbent assays (ELISA) can be used for protein identification but only when paired with antibodies for the target of interest.[4] Protein mass spectrometry is a powerful tool for identification but requires specialized training and expensive equipment. These factors make Western blots and mass spectrometry impractical for the majority of point-of-care and consumer-level applications. The ideal protein assay would permit concurrent protein identification and quantification while reducing overall cost and complexity.

Gold nanoparticles are a common platform for emerging nanobiosensors because of their unique optical properties and functionalizability.[5−7] Localized surface plasmon resonance (LSPR) of gold nanoparticles lends these solutions a variety of colors from orange-red to purple-blue, depending on particle size and shape.[8] Particle aggregation causes plasmon coupling, and the resulting shift in color can be visible to the unaided eye.[9] Several studies have shown how colloidal stability of gold nanoparticles can be controlled with functionalized aptamers, peptides, or antibodies to detect whole cells,[10] proteins,[11] nucleic acids,[12] and small molecules.[13,14] While these systems offer excellent specificity due to their "lock and key" design, high synthesis complexity and probe cost limit their usefulness for broad-spectrum protein sensing.

Proteins in solution can adsorb onto nanoparticles and induce changes in colloidal stability without the need for specific probes.[15−17] Particle size,[18−21] shape,[22−24] surface coating,[15,17,25,26] and charge[25,27] are all thought to affect these colloidal interactions, and the resultant effects on particle aggregation. Single-nanoparticle systems for protein quantification have been demonstrated based on this phenomenon, where the adsorption of proteins to gold nanoparticles changes their colloidal stability.[28−30] One group has even shown the ability to distinguish between different protein conformations.[31] The advantages of these systems over probe-based systems are lower synthesis cost and the ability to detect a wide variety of proteins. By preparing an array of different nanoparticles that

Received: April 7, 2016
Revised: June 17, 2016
Published: July 11, 2016

DOI: 10.1021/acs.langmuir.6b01339
Langmuir 2016, 32, 7621−7629

respond differently to the same analyte, a "chemical nose" type sensor could generate a unique fingerprint for each analyte.[32−35] Compared with other multiplexed systems that use displacement of quenched green fluorescent protein (GFP),[36] monitoring the absorbance spectrum and aggregation of gold nanoparticles does not require the use of expensive fluorophores or a fluorescence spectrometer. While any given response is nonspecific and would not itself allow for identification, an array of nonspecific responses can generate an identifiable pattern. Furthermore, extending the array to include many different nonspecific indicators will enhance specificity based on the "chemical nose" model. To account for variability between applications, machine learning can be used to train these "chemical nose" biosensors on known samples for specific applications (i.e., samples with known concentrations of proteins). The observed responses to known samples can then be used to identify unknown samples using techniques such as linear discriminant analysis, as previously shown with ocular pathogens.[33]

While many different aspects of gold colloid stability have been studied, the role of surfactants on protein−nanoparticle interactions is frequently overlooked. It is well known that surfactants can change nanoparticle surface properties and induce protein denaturation. Many ionic surfactants such as sodium dodecyl sulfate (SDS) and cetyltrimethylammonium bromide (CTAB) are strong denaturing agents.[37−39] Nonionic surfactants such as Triton X and TWEEN 20 (polysorbate 20) generally do not denature proteins.[37,40] The degree to which a protein is denatured depends on many factors including charge, hydrophobicity, and structure of the protein and surfactant.[37,41] Protein denaturation can also affect protein−nanoparticle interactions by changing the number and nature of binding sites, whether they are hydrophobic regions, charged regions, or exposed thiol groups.[31] It is therefore likely that surfactant type can influence gold nanoparticle−protein interactions and govern their colloidal stability. To our knowledge, no study has leveraged these differences for protein detection and identification. In this investigation, we demonstrate how the use of different surfactants to stabilize gold nanoparticles can affect protein-induced aggregation. We also demonstrate how several different proteins can be visually distinguished at nanomolar concentrations based on their unique response to three different surfactant−nanoparticle combinations. Finally, we show how varying the surfactant concentration can change the sensitivity across a range of protein concentrations, allowing for colorimetric assays with adjustable linear ranges. While an in-depth characterization of aggregation mechanisms may help in refining and optimizing this technique, the observation that different protein samples produce differential response in gold nanoparticle solutions allows for "chemical nose" classification of protein samples. These findings have implications beyond the biosensor application, wherever the influence of biomolecules on gold nanoparticle stability may alter their behavior.

METHODS

Materials. Gold(III) chloride hydrate ($HAuCl4{\cdot}xH_2O$), CTAB, sodium borohydride, silver nitrate, hydrochloric acid, nitric acid, sodium hydroxide, L-ascorbic acid, SDS, TWEEN 20, bovine serum albumin (BSA) (A2153), albumin from human serum (HSA) (A1653), immunoglobulin G from human serum (IgG) (I4506), human hemoglobin (Hgb) (H7379), and lysozyme from chicken egg white (Lyz) (L6876) were purchased from Sigma-Aldrich (Oakville, ON, Canada). 400 mesh Formvar/carbon-coated copper grids were purchased from Canemco (Gore, QC, Canada). Trisodium citrate dihydrate and BupH phosphate-buffered saline packs were purchased from Thermo Fisher Scientific (Burlington, ON, Canada). Sterile UV-star 96-well microplates, scintillation vials (20 mL), sodium chloride (ACS grade), Nalgene sterilization filter units (0.2 μm pore size), 15 mL polypropylene centrifuge tubes, and 1.7 mL polypropylene microcentrifuge tubes were purchase from VWR (Mississauga, ON, Canada). All procured chemicals were used without further purification. The 20 mL vials used for gold nanoseed synthesis were cleaned using 12 M sodium hydroxide, and larger glassware was cleaned using aqua regia as described in a previously published protocol.[42] Water used for the preparation of solutions was purified using a Millipore water filtration system to an electrical resistivity greater than 15 MΩ·cm. All other glass vials were triple-rinsed with Millipore water and dried completely prior to use.

Gold Nanoparticle Synthesis. Spherical CTAB-coated gold nanoparticles were synthesized according to a previously published protocol.[43] All synthesis solutions were prepared in Millipore water (>15 MΩ·cm). In brief, gold seed precursor was prepared by adding 60 μL of ice-cold sodium borohydride to a solution containing 18.812 mL of Millipore water, 188 μL of 10 mg/mL gold(III) chloride, and 1 mL of 2 mM trisodium citrate under vigorous stirring. Following the addition of sodium borohydride, the solution was stirred for 1 min and left to mature overnight under dark ambient conditions. Nanoparticle growth solution was prepared under moderate stirring by adding 8.974 mL of 11 mM gold chloride, 1.344 mL of 5 mM silver nitrate, and 1.442 mL of 100 mM L-ascorbic acid to 210 mL of 1.47 mM CTAB. Finally, 5.6 mL of gold seed precursor was added to the solution and stirred for an additional 1.5 min, at which point the solution was incubated overnight under dark ambient conditions. The final nanoparticle solution was pelleted via centrifugation and resuspended in 1 mM CTAB solution. These synthesis conditions were previously shown to produce spherical gold nanoparticles approximately 32 nm in diameter.[43] Dynamic light scattering (DLS) results confirmed that the mean diameter of gold nanoparticles used in this study was between 32 and 35 nm (Table S2).

Surfactant Exchange. TWEEN-20- and SDS-stabilized nanoparticles were prepared from CTAB-stabilized nanoparticles by repeated washing and surfactant replacement. Parts of this procedure were adapted from Tebbe et al.,[44] wherein CTAB was displaced from gold nanoparticles by BSA. Here gold nanoparticles suspended in 1 mM CTAB were added dropwise under ultrasonication to an equal volume of the new concentrated surfactant (100 mM TWEEN 20 or 100 mM SDS). Solutions were then sonicated for an additional 2 min prior to centrifugation for 15 min at 10 000 rpm. The supernatant was discarded and the nanoparticle pellets were resuspended and sonicated in a 1 mM solution of the new surfactant. This centrifugation and resuspension process was repeated twice, with the final resuspension being in half the supernatant volume to regain original particle concentration. Following surfactant exchange, nanoparticles were suspended in 1 mM solutions of SDS, TWEEN 20, or CTAB, and no excess surfactant was removed. Nanoparticles were then characterized and tested for stability in PBS.

Gold nanoparticle solutions with different CTAB concentrations were prepared by centrifuging particles for 15 min at 10 000 rpm, discarding the supernatant, and resuspending the nanoparticles in a higher or lower concentration of CTAB. This wash step was repeated twice to bring the new CTAB concentration as close as possible to the nominal value.

Gold Nanoparticle Characterization. Characterization of gold nanoparticles was performed using ultraviolet−visible (UV−vis) spectroscopy, zeta potential, and DLS measurement. Absorbance spectra were collected from 300 to 900 nm, at 1 nm increments, on 300 μL samples in 96-well plates using an Epoch microplate spectrophotometer (Winooski, VT). Zeta potential and DLS measurements were performed concurrently using a Malvern Zetasizer. Prior to DLS and zeta potential measurement, samples were diluted 1:2 in 1/4× PBS (pH 7.4) to match experimental ionic conditions.

DOI: 10.1021/acs.langmuir.6b01339
Langmuir 2016, 32, 7621−7629

Table 1. Surfactant Structures and Zeta Potentials of Gold Nanoparticles after Being Stabilized with 1 mM CTAB, 1 mM TWEEN 20, or 1 mM SDS[a]

Surfactant	Structure	Type	NP Zeta Potential (pH 7.4)
CTAB	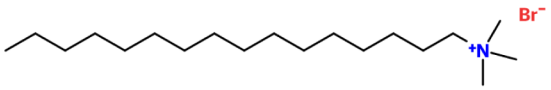	Cationic	25.7 mV
TWEEN® 20	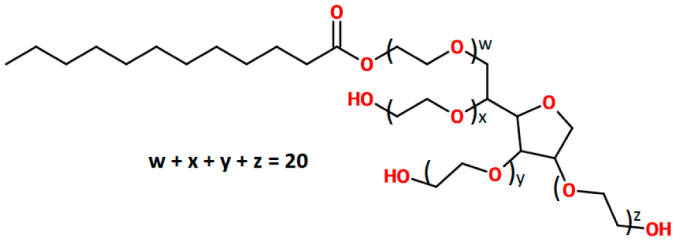	Non-ionic	-16.2 mV
SDS	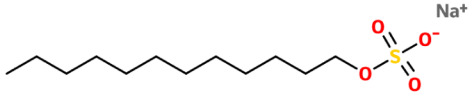	Anionic	-46.5 mV

[a]Zeta potentials measured following 1:2 dilution in 1/4× PBS (pH 7.4).

Preparation of Protein Solutions. Fresh protein solutions were prepared prior to each experiment from lyophilized powder as per supplier's instructions. These proteins were selected in part due to their clinical significance[45,46] and presence in common laboratory samples as well as their differences in size and isoelectric points. Reconstitution was performed by weighing out the lyophilized powder in a microcentrifuge tube and adding the appropriate amount of sterile solvent (1/4× PBS). Gentle inversion was used to promote protein dissolution and prevent denaturation from shear stress due to vortexing. Following reconstitution, protein concentrations were verified and adjusted as necessary based on A_{280} measurements. The Beer–Lambert Law was used to calculate molar concentrations from absorbance values using absorption parameters from the supplier (or literature where supplier values were not available) (Table S1)

$$A = \varepsilon \times l \times c$$

where A is the optical density of the sample, ε is the molar absorption coefficient of the protein, l is the optical path length, and c is the molar concentration of the protein solution. Serial dilutions were performed to achieve protein concentrations below the linear range of the Epoch microplate spectrophotometer (0.1–2.0). Protein concentrations for samples outside this range were extrapolated from the closest dilution with a reliable absorbance value. To obtain a final concentration of 150 nM, solutions were first normalized using A_{280} to a concentration of 4.5 μM. Samples were then diluted 10× to achieve a concentration of 450 nM. Following the addition of 200 μL of gold nanoparticle solution to 100 μL of 450 nM protein solution, the final protein concentration was 150 nM.

Protein–Gold Incubation. Concentration-dependent response and protein identification experiments were assessed spectrophotometrically in a transparent 96-well plate. 100 μL of each protein sample or solvent control was added to the 96-well plate. 200 μL of the gold nanoparticle solution was then added to each well containing protein or control solution. Eight replicates were used for each protein–surfactant combination during protein discrimination at 150 nM. Plates were then placed on a Stovall Belly Dancer orbital shaker (Peosta, IA) for 2 min prior to 20 h of incubation in the dark at room temperature. Following incubation, spectral scans for each well containing gold nanoparticles were obtained from 300 to 900 nm, in increments of 1 nm.

Data Analysis. Normalized response was defined as a change in peak height relative to the solvent control. First, the position (in nanometers) of the control absorbance peak was determined. Absorbance values at that wavelength were then recorded for all samples. Baseline absorbance at 800 nm was then determined for each sample, including solvent controls. Peak height was calculated by subtracting the sample's baseline absorbance (800 nm) from the sample's absorbance corresponding to the control peak position (eq 1). Peak heights were then normalized against the control to obtain a normalized response for each protein sample (eq 2).

Protein classification was done in R using the FactoMineR package for Multiple Factor Analysis.[47] Each protein assayed consisted of three data sets (one spectrum for each surfactant). Each spectrum was treated as a separate category in MFA analysis. All figures were plotted using OriginPro. Photographs were taken using a Canon EOS Rebel T3 digital camera.

RESULTS AND DISCUSSION

Surfactant Exchange. We prepared three nanoparticle solutions, each with a different surfactant to study the surfactant's effect on the colloidal stability of gold nanoparticles. The cationic surfactant CTAB was used to stabilize nanoparticles during their synthesis. A 1 mM surfactant concentration was chosen based on preliminary experiments because this value was close to the minimum concentration required to maintain colloidal stability in saline. TWEEN 20 and SDS were chosen as model nonionic and anionic surfactants, respectively. A common strategy for displacement of CTAB takes advantage

DOI: 10.1021/acs.langmuir.6b01339
Langmuir 2016, 32, 7621–7629

of strong thiol−gold interactions;[48] however, displacement by nonthiolated molecules is possible. It has recently been confirmed through surface-enhanced Raman spectroscopy (SERS) that complete displacement of CTAB by BSA on the surface of gold nanoparticles can be achieved without nanoparticle aggregation.[44] Using a similar strategy, dropwise addition of CTAB-coated nanoparticles into high concentrations of TWEEN 20 or SDS while under ultrasonication was found to produce stable nanoparticles with negligible changes in absorption spectra. When resuspended in 1 mM solutions of their respective surfactant, these solutions were also stable under moderate ionic conditions (addition of 100 μL of 1/4× PBS to 200 μL of nanoparticle solution).

CTAB is a cationic surfactant due to its quaternary ammonium cation. As a result, CTAB-stabilized gold nanoparticles are cationic.[43] Because of the nonionic and anionic nature of TWEEN 20 and SDS, respectively, nanoparticles coated with these surfactants should adopt neutral and negative zeta potentials at pH 7.4. The results of zeta potential measurements at pH 7.4 are shown in Table 1. Reversal of zeta potential from +25.7 mV for CTAB-stabilized particles to −46.5 mV for SDS-stabilized particles matches the predicted outcome based on surfactant charge. While nanoparticles stabilized with nonionic TWEEN 20 still possessed an electrostatic potential of approximately −16.2 mV, the polarity was inverted compared with CTAB-stabilized particles, and the magnitude of this potential was smaller than that of anionic SDS. Despite predictions of a neutral particle given to the anionic nature of TWEEN 20, these results reflect other studies where zeta potential of TWEEN-20-coated gold nanoparticles was studied.[49−51]

The process of surfactant exchange instead of de novo synthesis with different surfactants was chosen to preserve the size and morphology of the gold cores, as both of these parameters can impact nanoparticle−protein interactions. DLS results indicate that the average particle diameters were similar (Table S2). Slight variations were likely due to minor aggregation during the washing and centrifugation process.

This exchange of surfactant from one type to another is useful for nanoparticle characterization because it allows each nanoparticle variety to use the same gold core. While synthesis of similar nanoparticles can be achieved using different surfactants, maintaining interbatch reproducibility while changing surfactant type would require extensive tuning and quality control or specialized purification. Using gold cores from a single process and replacing the surfactant postsynthesis helps control interbatch variability. This technique also allows nanoparticle morphologies synthesized in a nonbiocompatible surfactant to be adapted for use in vivo. It is interesting to note that gold nanoparticles with anionic side chains are generally considered less toxic than their cationic counterparts.[52] Furthermore, nonionic surfactants and particularly the polyoxyethylene sorbitan family (i.e., TWEEN) have lower skin toxicity than both cationic and anionic surfactants.[53] As a result, a similar surfactant exchange strategy could be used to produce surfactant-stabilized gold nanoparticles where CTAB toxicity is of concern.

Protein Identification. Because of aggregation-dependent changes in color, the effects of proteins on gold nanoparticle stability can be monitored visually or using a spectrophotometer. In some cases, the addition of proteins has been shown to induce aggregation in a concentration-dependent response.[22,30,31] Other studies have shown that the addition of proteins can actually stabilize gold nanoparticles against harsh environments (e.g., high salt conditions).[44,54] These observations are dependent on many factors including particle size,[18−21] shape,[22−24] and charge.[25,27] When multiple proteins were assessed, the observed changes in absorption spectrum were also dependent on the protein identity.[24,55]

To assess whether proteins can be discriminated based on their interaction with surfactants, we incubated five 150 nM protein solutions (BSA, HSA, Hgb, IgG, and Lyz) with each surfactant−nanoparticle combination and characterized their UV−vis absorption spectra. Solutions were incubated overnight under dark ambient conditions to allow solutions ample time for color change; however, samples were noticeably different within 1 min of incubation. The final appearance of each well is shown in Figure 1. In many cases, clear differences between the

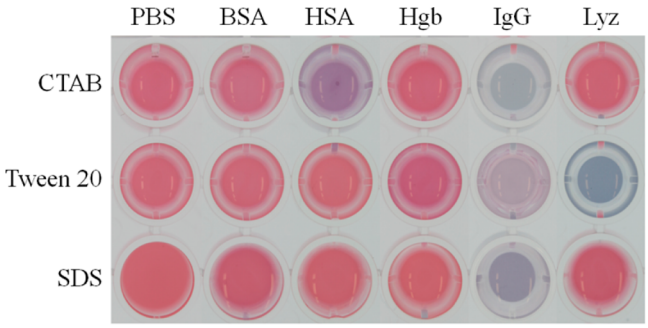

Figure 1. Visual appearance of gold nanoparticles with different 1 mM surfactants after 20 h of incubation with 150 nM BSA, HSA, Hgb, IgG, Lyz, or 1/4× PBS (negative control).

proteins were apparent. While the responses of BSA, Hgb, and PBS appeared similar to the unaided eye, they could be distinguished based on spectrophotometric data (Figure 2). Preliminary experiments in CTAB showed a concentration-dependent response to HSA and BSA from 27.46 nM to 450 μM; however, Lyz did not induce a response at any tested concentration. Unlike the response observed in CTAB, Lyz caused extensive color shifts in TWEEN 20 particles, whereas HSA and BSA did not. These changes in color correspond to red-shifting and peak broadening in the absorption spectra (Figure 2A−C) and support the notion that the surfactant type plays a key role in modulating nanoparticle stability.

One of the main protein characteristics believed to alter protein−nanoparticle interactions is relative charge of proteins and nanoparticles.[29,56] Lyz and IgG have isoelectric points of 11.0 and 8.0, respectively (Table S1). Therefore, under experimental conditions (pH 7.4), Lyz is positively charged and IgG is slightly positive. The positive charge of lysozyme may explain the stability of positively charged CTAB-coated gold nanoparticles due to mutual repulsion, however BSA (pI 5.1) and Hgb (pI 6.8), which are negatively charged at pH 7.4 only caused minor aggregation. More aggregation was observed with HSA (pI 5.2) than BSA, despite these two proteins having nearly identical pIs. Furthermore, positively charged Lyz induced more aggregation in slightly negative TWEEN-20-coated nanoparticles than the highly negative SDS-coated nanoparticles. Therefore, the relative charge of gold nanoparticles and proteins is insufficient to explain differences in stability. In addition to adsorption-driven aggregation, several studies have shown that nonadsorptive depletion effects of polyethylene glycol (PEG)[57] and proteins[58] can alter the

DOI: 10.1021/acs.langmuir.6b01339
Langmuir 2016, 32, 7621−7629

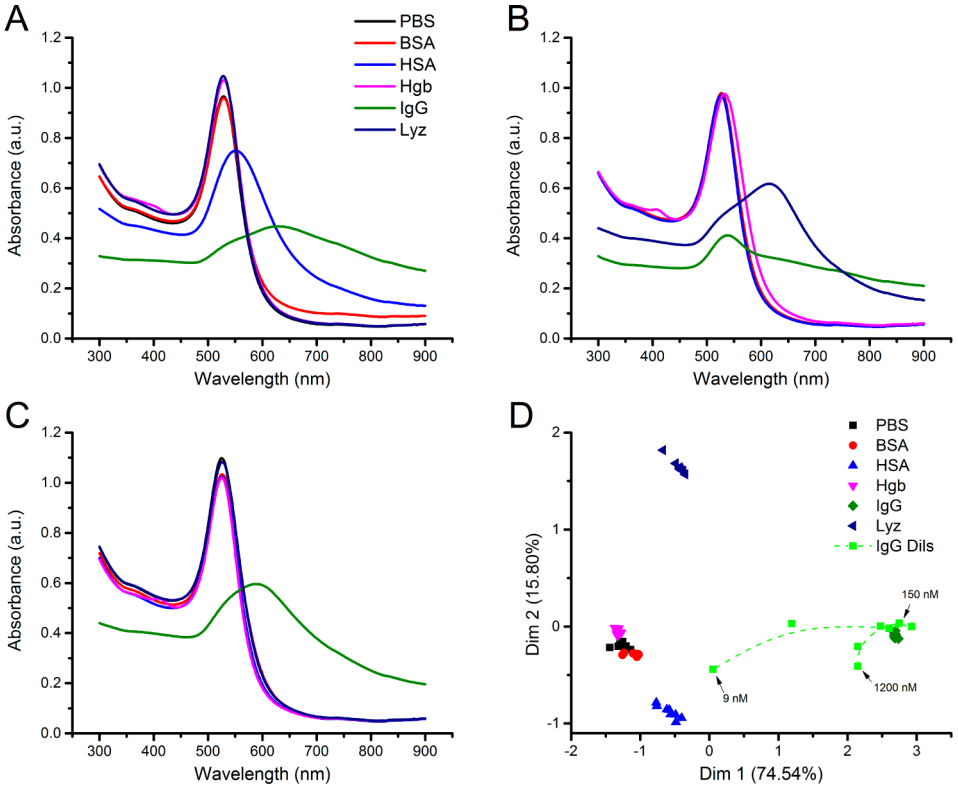

Figure 2. Differential response of gold nanoparticles to five different proteins at 150 nM. Average UV−vis absorption spectra (n = 8) are shown for (A) CTAB-stabilized nanoparticles, (B) TWEEN-20-stabilized nanoparticles, and (C) SDS-stabilized nanoparticles. (D) Multiple factor analysis (MFA) plot for the combined response of all three nanoparticles to each protein at 150 nM. A b-spline curve (green dash) is shown to help visualize the concentration gradient for IgG dilutions (IgG Dils) from 1200 to 9 nM.

colloidal stability of gold nanoparticles. This mechanism may be particularly relevant in cases with negligible protein adsorption. Because of the role of protein size and electrostatic potential in determining the strength of depletion forces,[58] it is likely that this mechanism can contribute to protein identification based on observed changes in colloidal stability. As such, an in-depth investigation of parameters influencing adsorptive- and depletion-driven aggregation is underway to improve protein discrimination.

Multiple factor analysis (MFA) was performed on the full set of UV−vis absorption curves following the 20 h incubation period. MFA was chosen because this extension of principal component analysis (PCA) allows each nanoparticle spectrum (CTAB, TWEEN 20, and SDS) to be treated as a distinct set of variables (i.e., separate features of the fingerprint). In this case, each surfactant−nanoparticle combination was treated as a separate data set with 48 samples (8 replicates × 5 proteins and 1 negative control). The data from IgG dilutions were also included, from 1200 to 9 nM, to highlight the effect of protein concentration. The resultant biplot is shown in Figure 2D.

The MFA biplot of five proteins and one negative control shows grouping and separation of samples based on their protein identities. The largest separation was observed for HSA, IgG, and Lyz, as these proteins produced large spectral shifts in at least one surfactant−particle combination. Weaker responses for BSA and Hgb result in grouping closer to the control; however, some clustering and separation is still evident. The two principal components identified using this method could account for 90.34% of observed variability between samples.

Concentration-Dependent Response. IgG solutions were prepared at several concentrations to observe how protein concentration affects spectral response for the three surfactants. The resultant UV−vis absorption curves are shown in Figure 3. As concentration increases from 9.4 to 37.5 nM, we see a decrease in absorbance for CTAB and TWEEN-20-stabilized nanoparticles (Figure 3A,B). At higher concentrations (75 to 1200 nM) absorbance of CTAB-stabilized particles increases but the peak remains broad. Similarly, TWEEN-20-stabilized particles increase in absorbance slightly at higher concentrations but maintain a relatively narrow peak. In neither case is the original absorbance peak regained at high protein concentrations. For SDS-stabilized nanoparticles (Figure 3C), as IgG concentration increases from 9.4 to 600 nM, we see an increase in absorbance, contrary to the trend for CTAB and TWEEN 20. Absorbance then decreases slightly as IgG concentration increases from 600 to 1200 nM. Even at the lowest IgG concentration assayed, significant spectral shifts and broadening were observed. The trends of increasing and decreasing absorbance as protein concentration changes reflect previous observations that nanoparticles can enter different regimes of stability depending on protein concentration.[59]

The spectra in Figure 3 were analyzed using MFA and plotted alongside the 150 nM protein samples (Figure 2D). A b-spline curve is shown to help visualize the dilution order. The 150 nM sample agrees with previously collected replicates, indicating good reproducibility. Higher and lower dilutions of IgG indicate that the position of samples on the MFA plot relative to the PBS control is concentration-dependent. While a change in direction around 150 nM reflects the bell-shaped response, performing the assay in the linear range would allow for concurrent identification and quantification. Furthermore, noticeable spectral broadening of SDS-stabilized particles with

DOI: 10.1021/acs.langmuir.6b01339
Langmuir 2016, 32, 7621−7629

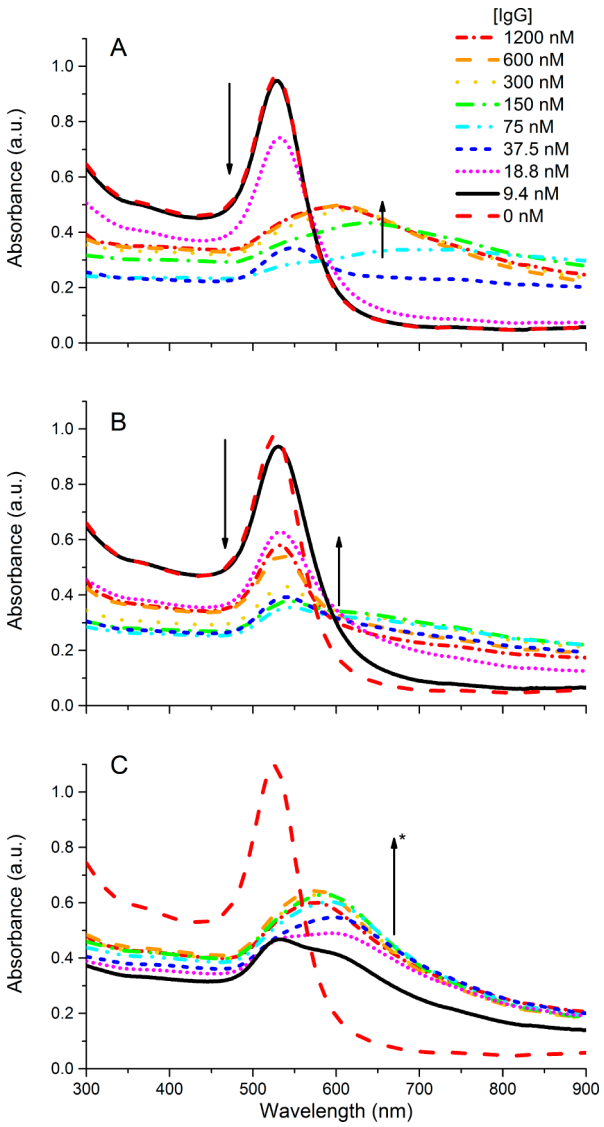

Figure 3. Changes in UV−vis absorption curves of gold nanoparticles in response to different IgG concentrations. Nanoparticles were suspended in (A) 1 mM CTAB, (B) 1 mM Tween 20, and (C) 1 mM SDS. Arrows indicate the trend in absorption following increases in protein concentration. In panel C, asterisk (*) indicates a decrease in absorbance as concentration increases from 600 to 1200 nM, contrary to the overall trend.

9.4 nM IgG suggests the potential for lower concentrations to induce changes as well; therefore, the detection limit for certain proteins may be significantly lower than 9.4 nM.

CTAB Concentration. Previous studies have shown that CTAB concentration affects the extent of BSA and HSA denaturation.[39,60] Because BSA conformation affects the extent of nanoparticle aggregation,[31] it is evident that surfactant concentration should be investigated as a means of controlling the extent of nanoparticle aggregation and may be useful for developing colorimetric assays. To assess how different concentrations of surfactant affect the protein concentration-dependent response of gold nanoparticles, we prepared CTAB-stabilized gold nanoparticles in seven different dilutions of CTAB ranging from 50 to 0.78 mM. Lower concentrations of CTAB were not used due to particle instability under working salt conditions. We used BSA and CTAB as models due to previous studies that characterized CTAB-dependent denaturation of BSA.[60] The normalized sample response was defined as a peak-height difference between sample and control UV−vis absorption spectra (eqs 1 and 2). Peak-height refers to the difference in absorbance between the characteristic peak wavelength for dispersed nanoparticles and a long-wavelength baseline (800 nm). As is typical with gold nanoparticles, aggregation results in decreased absorbance at the peak wavelength and higher absorbance at longer wavelengths.[35] The normalized response compares this peak height to the peak height of nonaggregated samples to quantify the change in aggregation. The resultant concentration-dependent curves are shown in Figure 4.

$$height_{sample} = A_{sample}(1^\circ \text{ peak position}) - A_{sample}(800\ \text{nm}) \quad (1)$$

$$\text{normalized sample response} = height_{control} - height_{sample} \quad (2)$$

Several different papers have observed positive,[24,28,61] negative,[31,62] and nonlinear[21,63] (e.g., bell-shaped) correlations between protein concentration and nanoparticle stability. For bell-shaped response curves, it has been proposed that particles pass through several regimes of stability as protein concentration increases.[59] At low concentrations, protein concentration is too low to induce nanoparticle aggregation. An increase in protein concentration induces large nanoparticle aggregates to form. If nanoparticles are exposed instantaneously to sufficiently high protein concentrations, the surface becomes saturated with protein and a large protein corona provides steric stabilization, thereby preventing aggregation. This behavior was only recently described with polystyrene.[59] The work by Cukalevski et al. relates this response to the number of IgG molecules per polystyrene nanoparticle. While their nanoparticles were devoid of surfactant, it is clear from Figure 4 that this relationship is also sensitive to surfactant concentration. A general trend emerges in Figure 4A, whereby increasing CTAB concentrations shift the response curve toward higher protein concentrations. In other words, higher protein concentrations are required to induce aggregation under higher CTAB concentrations. In Figure 4B, we see that this relationship scales by approximately $\sqrt{\text{CTAB}}$ to BSA. Ongoing studies are investigating whether this behavior is due to competition at the gold surface between CTAB and BSA or whether denaturation of BSA by CTAB is an important step in gold nanoparticle aggregation; however, both mechanisms may allow for tuning of sensitivity and linear range in a surfactant-based gold nanoparticle protein sensor. Finally, we also note the presence of a dual-peak in the concentration-dependent response curve, the cause of which is subject to ongoing investigations.

■ CONCLUSION

The effects of proteins on gold nanoparticle stability and resultant changes in absorption spectra are frequently studied for applications in biomolecular sensing. Using a simple washing procedure, we have prepared several stable gold nanoparticles in cationic, nonionic, and anionic solutions. This surfactant exchange procedure resulted in nanoparticles with varying zeta potential and maintained their stability under moderate ionic conditions. By incubating these gold nanoparticles with different proteins, we have shown how the identity and concentration of a surfactant can change the particle aggregation behavior. We have also demonstrated how

DOI: 10.1021/acs.langmuir.6b01339
Langmuir 2016, 32, 7621−7629

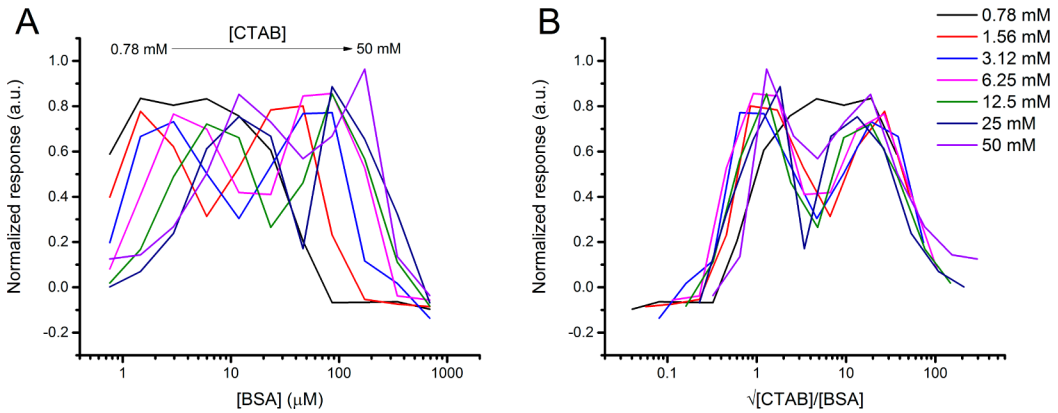

Figure 4. Concentration-dependent response of gold nanoparticles to BSA when suspended in varying concentrations of CTAB. Normalized response is plotted against (A) concentration of BSA in μM and (B) the ratio of $\sqrt{\text{CTAB}}$ to BSA.

differences in response produce a unique color and UV−vis absorption pattern for each protein, allowing for rapid visual protein identification. The effects of surfactants on nanoparticle response to proteins can therefore be exploited for multiplexed protein assays. Finally, we have shown how surfactant-coated gold nanoparticles can be a tool for studying interactions between nanoparticles and other biomolecules. Ongoing projects include kinetic studies to further elucidate the role of surfactant on aggregation, investigations into the effects of different chemical and physical parameters on the aggregation mechanism, and determining whether the observed responses can be extended to identify or group proteins based on their families.

■ ASSOCIATED CONTENT

Supporting Information

The Supporting Information is available free of charge on the ACS Publications website at DOI: 10.1021/acs.langmuir.6b01339.

Table S1. Physical and optical parameters of proteins prepared in solution. Table S2. DLS measurements for gold nanoparticles suspended in CTAB, Tween 20, or SDS. (PDF)

■ AUTHOR INFORMATION

Corresponding Author

*Tel: +1 519-888-4567, ext. 38605. Fax: +1 519-888-4347. E-mail: frank.gu@uwaterloo.ca.

Author Contributions

The manuscript was written through contributions of all authors. All authors have given approval to the final version of the manuscript.

Notes

The authors declare no competing financial interest.

■ ACKNOWLEDGMENTS

This work was financially supported by the Natural Sciences and Engineering Research Council of Canada (NSERC) and 20/20 NSERC − Ophthalmic Materials Network. We thank Professor Pu Chen for providing his Zetasizer and for help with zeta potential measurements. J.L.R. is grateful for the NSERC Canada Graduate Research Scholarship − Master's and for the Waterloo Institute for Nanotechnology (WIN) Nanofellowship. M.S.V. is grateful for the NSERC Vanier Graduate Scholarship and the Banting Postdoctoral Fellowship.

■ ABBREVIATIONS

BCA	bicinchoninic acid assay
PAGE	polyacrylamide gel electrophoresis
ELISA	enzyme-linked immunosorbent assay
LSPR	localized surface plasmon resonance
BSA	bovine serum albumin
HSA	human serum albumin
IgG	immunoglobulin G
Lyz	lysozyme
Hgb	hemoglobin
NP	nanoparticle
CTAB	cetyltrimethylammonium bromide
SDS	sodium dodecyl sulfate
GFP	green fluorescence protein
DLS	dynamic light scattering
UV−vis	ultraviolet−visible
SERS	surface-enhanced Raman spectroscopy
PCA	principal component analysis
MFA	multiple factor analysis
PBS	phosphate-buffered saline
OD	optical density

■ REFERENCES

(1) Rusling, J. F.; Kumar, C. V.; Gutkind, J. S.; Patel, V. Measurement of Biomarker Proteins for Point-of-Care Early Detection and Monitoring of Cancer. *Analyst* **2010**, *135* (10), 2496−2511.

(2) Fasano, A.; Catassi, C. Current Approaches to Diagnosis and Treatment of Celiac Disease: An Evolving Spectrum. *Gastroenterology* **2001**, *120* (3), 636−651.

(3) Anderson, N. L. The Clinical Plasma Proteome: A Survey of Clinical Assays for Proteins in Plasma and Serum. *Clin. Chem.* **2010**, *56* (2), 177−185.

(4) Towbin, H.; Staehelin, T.; Gordon, J. Electrophoretic Transfer of Proteins from Polyacrylamide Gels to Nitrocellulose Sheets: Procedure and Some Applications. *Proc. Natl. Acad. Sci. U. S. A.* **1979**, *76* (9), 4350−4354.

(5) Verma, M. S.; Rogowski, J. L.; Jones, L.; Gu, F. X. Colorimetric Biosensing of Pathogens Using Gold Nanoparticles. *Biotechnol. Adv.* **2015**, *33* (6), 666−680.

(6) Wang, J.; Qu, X. Recent Progress in Nanosensors for Sensitive Detection of Biomolecules. *Nanoscale* **2013**, *5* (9), 3589−3600.

(7) Bellan, L. M.; Wu, D.; Langer, R. S. Current Trends in Nanobiosensor Technology. *Wiley Interdiscip. Rev. Nanomed. Nanobiotechnol.* **2011**, *3* (3), 229−246.

DOI: 10.1021/acs.langmuir.6b01339
Langmuir 2016, 32, 7621−7629

(8) Jain, P. K.; Lee, K. S.; El-Sayed, I. H.; El-Sayed, M. A. Calculated Absorption and Scattering Properties of Gold Nanoparticles of Different Size, Shape, and Composition: Applications in Biological Imaging and Biomedicine. *J. Phys. Chem. B* **2006**, *110* (14), 7238−7248.
(9) Ghosh, S. K.; Pal, T. Interparticle Coupling Effect on the Surface Plasmon Resonance of Gold Nanoparticles: From Theory to Applications. *Chem. Rev.* **2007**, *107* (11), 4797−4862.
(10) Wang, S.; Singh, A. K.; Senapati, D.; Neely, A.; Yu, H.; Ray, P. C. Rapid Colorimetric Identification and Targeted Photothermal Lysis of Salmonella Bacteria by Using Bioconjugated Oval-Shaped Gold Nanoparticles. *Chem. - Eur. J.* **2010**, *16* (19), 5600−5606.
(11) Chandrawati, R.; Stevens, M. M. Controlled Assembly of Peptide-Functionalized Gold Nanoparticles for Label-Free Detection of Blood Coagulation Factor XIII Activity. *Chem. Commun.* **2014**, *50* (41), 5431−5434.
(12) Gill, P.; Alvandi, A.-H.; Abdul-Tehrani, H.; Sadeghizadeh, M. Colorimetric Detection of Helicobacter Pylori DNA Using Isothermal Helicase-Dependent Amplification and Gold Nanoparticle Probes. *Diagn. Microbiol. Infect. Dis.* **2008**, *62* (2), 119−124.
(13) Xiao, Q.; Gao, H.; Lu, C.; Yuan, Q. Gold Nanoparticle-Based Optical Probes for Sensing Aminothiols. *TrAC, Trends Anal. Chem.* **2012**, *40*, 64−76.
(14) Guo, Y.; Wang, Z.; Qu, W.; Shao, H.; Jiang, X. Colorimetric Detection of Mercury, Lead and Copper Ions Simultaneously Using Protein-Functionalized Gold Nanoparticles. *Biosens. Bioelectron.* **2011**, *26* (10), 4064−4069.
(15) Cui, M.; Liu, R.; Deng, Z.; Ge, G.; Liu, Y.; Xie, L. Quantitative Study of Protein Coronas on Gold Nanoparticles with Different Surface Modifications. *Nano Res.* **2014**, *7* (3), 345−352.
(16) Cedervall, T.; Lynch, I.; Lindman, S.; Berggård, T.; Thulin, E.; Nilsson, H.; Dawson, K. a; Linse, S. Understanding the Nanoparticle-Protein Corona Using Methods to Quantify Exchange Rates and Affinities of Proteins for Nanoparticles. *Proc. Natl. Acad. Sci. U. S. A.* **2007**, *104* (7), 2050−2055.
(17) Boulos, S. P.; Davis, T. a; Yang, J. A.; Lohse, S. E.; Alkilany, A. M.; Holland, L. a; Murphy, C. J. Nanoparticle-Protein Interactions: A Thermodynamic and Kinetic Study of the Adsorption of Bovine Serum Albumin to Gold Nanoparticle Surfaces. *Langmuir* **2013**, *29* (48), 14984−14996.
(18) Teichroeb, J. H.; Forrest, J. a; Jones, L. W. Size-Dependent Denaturing Kinetics of Bovine Serum Albumin Adsorbed onto Gold Nanospheres. *Eur. Phys. J. E: Soft Matter Biol. Phys.* **2008**, *26* (4), 411−415.
(19) Jiang, X.; Jiang, J.; Jin, Y.; Wang, E.; Dong, S. Effect of Colloidal Gold Size on the Conformational Changes of Adsorbed Cytochrome c: Probing by Circular Dichroism, UV-Visible, and Infrared Spectroscopy. *Biomacromolecules* **2005**, *6* (1), 46−53.
(20) De Paoli Lacerda, S. H.; Park, J. J.; Meuse, C.; Pristinski, D.; Becker, M. L.; Karim, A.; Douglas, J. F. Interaction of Gold Nanoparticles with Common Human Blood Proteins. *ACS Nano* **2010**, *4* (1), 365−379.
(21) Deng, Z. J.; Liang, M.; Toth, I.; Monteiro, M. J.; Minchin, R. F. Molecular Interaction of Poly(acrylic Acid) Gold Nanoparticles with Human Fibrinogen. *ACS Nano* **2012**, *6* (10), 8962−8969.
(22) Chaudhary, A.; Gupta, A.; Khan, S.; Nandi, C. K. Morphological Effect of Gold Nanoparticles on the Adsorption of Bovine Serum Albumin. *Phys. Chem. Chem. Phys.* **2014**, *16* (38), 20471−20482.
(23) Thioune, N.; Lidgi-Guigui, N.; Cottat, M.; Gabudean, A.-M.; Focsan, M.; Benoist, H.-M.; Astilean, S.; de la Chapelle, M. L. Study of Gold Nanorods−protein Interaction by Localized Surface Plasmon Resonance Spectroscopy. *Gold Bull.* **2013**, *46* (4), 275−281.
(24) Gagner, J. E.; Lopez, M. D.; Dordick, J. S.; Siegel, R. W. Effect of Gold Nanoparticle Morphology on Adsorbed Protein Structure and Function. *Biomaterials* **2011**, *32* (29), 7241−7252.
(25) Deng, Z. J.; Liang, M.; Toth, I.; Monteiro, M.; Minchin, R. F. Plasma Protein Binding of Positively and Negatively Charged Polymer-Coated Gold Nanoparticles Elicits Different Biological Responses. *Nanotoxicology* **2012**, *7* (3), 314−322.
(26) Dominguez-Medina, S.; McDonough, S.; Swanglap, P.; Landes, C. F.; Link, S. In Situ Measurement of Bovine Serum Albumin Interaction with Gold Nanospheres. *Langmuir* **2012**, *28* (24), 9131−9139.
(27) Brewer, S. H.; Glomm, W. R.; Johnson, M. C.; Knag, M. K.; Franzen, S. Probing BSA Binding to Citrate-Coated Gold Nanoparticles and Surfaces. *Langmuir* **2005**, *21* (20), 9303−9307.
(28) Ho, Y. T.; Poinard, B.; Yeo, E. L. L.; Kah, J. C. Y. An Instantaneous Colorimetric Protein Assay Based on Spontaneous Formation of a Protein Corona on Gold Nanoparticles. *Analyst* **2015**, *140* (4), 1026−1036.
(29) Wang, X.; Xu, Y.; Xu, X.; Hu, K.; Xiang, M.; Li, L.; Liu, F.; Li, N. Direct Determination of Urinary Lysozyme Using Surface Plasmon Resonance Light-Scattering of Gold Nanoparticles. *Talanta* **2010**, *82* (2), 693−697.
(30) Stoscheck, C. M. Protein Assay Sensitive at Nanogram Levels. *Anal. Biochem.* **1987**, *160* (2), 301−305.
(31) Deka, J.; Paul, A.; Chattopadhyay, A. Sensitive Protein Assay with Distinction of Conformations Based on Visible Absorption Changes of Citrate-Stabilized Gold Nanoparticles. *J. Phys. Chem. C* **2009**, *113* (17), 6936−6947.
(32) Verma, M. S.; Chen, P. Z.; Jones, L.; Gu, F. X. Controlling "chemical Nose" Biosensor Characteristics by Modulating Gold Nanoparticle Shape and Concentration. *Sens. Bio-Sensing Res.* **2015**, *5*, 13−18.
(33) Verma, M. S.; Chen, P. Z.; Jones, L.; Gu, F. X. Chemical Nose for the Visual Identification of Emerging Ocular Pathogens Using Gold Nanostars. *Biosens. Bioelectron.* **2014**, *61*, 386−390.
(34) Verma, M. S.; Tsuji, J. M.; Hall, B.; Chen, P. Z.; Forrest, J.; Jones, L.; Gu, F. X. Towards Point-of-Care Detection of Polymicrobial Infections: Rapid Colorimetric Response Using a Portable Spectrophotometer. *Sens. Bio-Sensing Res.* **2016**, *10*, 15.
(35) Verma, M. S.; Wei, S. C.; Rogowski, J. L.; Tsuji, J. M.; Chen, P. Z.; Lin, C. W.; Jones, L.; Gu, F. X. Interactions between Bacterial Surface and Nanoparticles Govern the Performance of "Chemical Nose" Biosensors. *Biosens. Bioelectron.* **2016**, *83*, 115−125.
(36) Moyano, D. F.; Rana, S.; Bunz, U. H. F.; Rotello, V. M. Gold Nanoparticle-Polymer/biopolymer Complexes for Protein Sensing. *Faraday Discuss.* **2011**, *152*, 33−42.
(37) Privé, G. G. Detergents for the Stabilization and Crystallization of Membrane Proteins. *Methods* **2007**, *41* (4), 388−397.
(38) Kelley, D.; McClements, D. J. Interactions of Bovine Serum Albumin with Ionic Surfactants in Aqueous Solutions. *Food Hydrocolloids* **2003**, *17* (1), 73−85.
(39) Vlasova, I. M.; Saletsky, a. M. Investigation of Denaturation of Human Serum Albumin under Action of Cethyltrimethylammonium Bromide by Raman Spectroscopy. *Laser Phys.* **2011**, *21* (1), 239−244.
(40) Seddon, A. M.; Curnow, P.; Booth, P. J. Membrane Proteins, Lipids and Detergents: Not Just a Soap Opera. *Biochim. Biophys. Acta, Biomembr.* **2004**, *1666*, 105−117.
(41) Gudiksen, K. L.; Gitlin, I.; Moustakas, D. T.; Whitesides, G. M. Increasing the Net Charge and Decreasing the Hydrophobicity of Bovine Carbonic Anhydrase Decreases the Rate of Denaturation with Sodium Dodecyl Sulfate. *Biophys. J.* **2006**, *91* (1), 298−310.
(42) Liu, J.; Lu, Y. Preparation of Aptamer-Linked Gold Nanoparticle Purple Aggregates for Colorimetric Sensing of Analytes. *Nat. Protoc.* **2006**, *1* (1), 246−252.
(43) Verma, M. S.; Chen, P. Z.; Jones, L.; Gu, F. X. Branching and Size of CTAB-Coated Gold Nanostars Control the Colorimetric Detection of Bacteria. *RSC Adv.* **2014**, *4* (21), 10660−10668.
(44) Tebbe, M.; Kuttner, C.; Männel, M.; Fery, A.; Chanana, M. Colloidally Stable and Surfactant-Free Protein-Coated Gold Nanorods in Biological Media. *ACS Appl. Mater. Interfaces* **2015**, *7* (10), 5984−5991.
(45) Shibutani, M.; Maeda, K.; Nagahara, H.; Ohtani, H.; Iseki, Y.; Ikeya, T.; Sugano, K.; Hirakawa, K. The Pretreatment Albumin to Globulin Ratio Predicts Chemotherapeutic Outcomes in Patients with Unresectable Metastatic Colorectal Cancer. *BMC Cancer* **2015**, *15*, 347.

DOI: 10.1021/acs.langmuir.6b01339
Langmuir 2016, 32, 7621−7629

(46) Manns, M. P.; Czaja, A. J.; Gorham, J. D.; Krawitt, E. L.; Mieli-Vergani, G.; Vergani, D.; Vierling, J. M. Diagnosis and Management of Autoimmune Hepatitis. *Hepatology* **2010**, *51* (6), 2193−2213.
(47) Lê, S.; Josse, J.; Husson, F. FactoMineR: An R Package for Multivariate Analysis. *J. Stat. Softw.* **2008**, *25* (1), 1−18.
(48) Liao, H.; Hafner, J. H. Gold Nanorod Bioconjugates. *Chem. Mater.* **2005**, *17* (19), 4636−4641.
(49) Bac, L. H.; Kim, J. S.; Kim, J. C. Size, Optical and Stability Properties of Gold Nanoparticles Synthesized by Electrical Explosion of Wire in Different Aqueous Media. *Rev. Adv. Mater. Sci.* **2011**, *28*, 117−121.
(50) Wang, X.; Wei, Y.; Wang, S.; Chen, L. Red-to-Blue Colorimetric Detection of Chromium via Cr (III)-Citrate Chelating Based on Tween 20-Stabilized Gold Nanoparticles. *Colloids Surf., A* **2015**, *472*, 57−62.
(51) Shih, Y. C.; Ke, C. Y.; Yu, C. J.; Lu, C. Y.; Tseng, W. L. Combined Tween 20-Stabilized Gold Nanoparticles and Reduced Graphite Oxide-Fe3O4 Nanoparticle Composites for Rapid and Efficient Removal of Mercury Species from a Complex Matrix. *ACS Appl. Mater. Interfaces* **2014**, *6* (20), 17437−17445.
(52) Goodman, C. M.; McCusker, C. D.; Yilmaz, T.; Rotello, V. M. Toxicity of Gold Nanoparticles Functionalized with Cationic and Anionic Side Chains. *Bioconjugate Chem.* **2004**, *15* (4), 897−900.
(53) Lémery, E.; Briançon, S.; Chevalier, Y.; Bordes, C.; Oddos, T.; Gohier, A.; Bolzinger, M.-A. Skin Toxicity of Surfactants: Structure/toxicity Relationships. *Colloids Surf., A* **2015**, *469*, 166−179.
(54) Dominguez-Medina, S.; Blankenburg, J.; Olson, J.; Landes, C. F.; Link, S. Adsorption of a Protein Monolayer via Hydrophobic Interactions Prevents Nanoparticle Aggregation under Harsh Environmental Conditions. *ACS Sustainable Chem. Eng.* **2013**, *1* (7), 833−842.
(55) Khandelia, R.; Deka, J.; Paul, A.; Chattopadhyay, A. Signatures of Specificity of Interactions of Binary Protein Mixtures with Citrate-Stabilized Gold Nanoparticles. *RSC Adv.* **2012**, *2* (13), 5617−5628.
(56) Pan, H.; Qin, M.; Meng, W.; Cao, Y.; Wang, W. How Do Proteins Unfold upon Adsorption on Nanoparticle Surfaces? *Langmuir* **2012**, *28* (35), 12779−12787.
(57) Zhang, X.; Servos, M. R.; Liu, J. Ultrahigh Nanoparticle Stability against Salt, pH, and Solvent with Retained Surface Accessibility via Depletion Stabilization. *J. Am. Chem. Soc.* **2012**, *134* (24), 9910−9913.
(58) Zhang, F.; Skoda, M. W. a; Jacobs, R. M. J.; Zorn, S.; Martin, R. a; Martin, C. M.; Clark, G. F.; Goerigk, G.; Schreiber, F. Gold Nanoparticles Decorated with Oligo(ethylene Glycol) Thiols: Protein Resistance and Colloidal Stability. *J. Phys. Chem. A* **2007**, *111* (49), 12229−12237.
(59) Cukalevski, R.; Ferreira, S. a.; Dunning, C. J.; Berggård, T.; Cedervall, T. IgG and Fibrinogen Driven Nanoparticle Aggregation. *Nano Res.* **2015**, *8* (8), 2733−2743.
(60) Vlasova, I. M.; Zhuravleva, V. V.; Saletskii, a. M. Denaturation of Bovine Serum Albumin under the Action of Cetyltrimethylammonium Bromide, according to Data from Fluorescence Analysis. *Russ. J. Phys. Chem. A* **2013**, *87* (6), 1027−1034.
(61) Gebauer, J. S.; Malissek, M.; Simon, S.; Knauer, S. K.; Maskos, M.; Stauber, R. H.; Peukert, W.; Treuel, L. Impact of the Nanoparticle-Protein Corona on Colloidal Stability and Protein Structure. *Langmuir* **2012**, *28* (25), 9673−9679.
(62) Chakraborty, S.; Joshi, P.; Shanker, V.; Ansari, Z. a; Singh, S. P.; Chakrabarti, P. Contrasting Effect of Gold Nanoparticles and Nanorods with Different Surface Modifications on the Structure and Activity of Bovine Serum Albumin. *Langmuir* **2011**, *27* (12), 7722−7731.
(63) Moerz, S. T.; Kraegeloh, A.; Chanana, M.; Kraus, T. Formation Mechanism for Stable Hybrid Clusters of Proteins and Nanoparticles. *ACS Nano* **2015**, *9* (7), 6696−6705.

DOI: 10.1021/acs.langmuir.6b01339
Langmuir 2016, 32, 7621−7629